



# Effect of Tailwater Height on Flow Performance of Sharp Crested Weir on Downstream Countercurrent in An Open Channel

Mohamad Nur Aliff Mohd Ali<sup>1</sup>, Mas Fawzi Mohd Ali<sup>1\*</sup>, Siti Natasha Malik Fesal<sup>1</sup>

<sup>1</sup>Faculty of Mechanical Engineering and Manufacturing,  
Universiti Tun Hussein Onn Malaysia, 86400 Parit Raja, Johor, MALAYSIA

\*Corresponding Author Designation

DOI: <https://doi.org/10.30880/rpmme.2022.03.01.042>

Received 15 Nov. 2021; Accepted 15 April 2022; Available online 30 July 2022

**Abstract:** Flow over low-head dams was complicated, and dangerous downstream rollers often develop. Particle-based flow visualization, a foundation for the preparatory work, and analysis of counter-current flow on the downstream were conducted. This study is to evaluate the relationship between upstream water level and tailwater height within the downstream counter-current existence. Variation of setup for height over the sharp-crested weir, ( $h/P$ ) 0.3, 0.4, 0.5, 0.6 and height of tailwater, ( $t_w/P$ ) 0.7, 0.8, 1.0 used. The result for velocity in X-direction for the dowel computed and plotted in contour graph show the different flow patterns and counter-current formation depend on ( $h/P$ ) and ( $t_w/P$ ).

**Keywords:** Sharp-Crested Weir, Counter-Current, Velocity Distribution, Dowel

## 1. Introduction

Weirs allow the water to pool behind them, thus enabling the water to spill continually over the top of the weir [1]. The term of weir may be used to refer to the crest of a spillway on a wide embankment dam. For example, in hydroelectric installations, spillways are needed as an outlet system to release water from the dam [2]. Low-head dams are common hydraulic structures that have historically been built to serve a wide variety of purposes [3]. Although these structures are comparatively small, they typically stand between 3 and 5 m in height and possessing a relatively calm and quiet nature. They have proved to be simply so-called drowning machines [4].

Sharp-crested weirs may be built in a range of shapes, such as rectangular, triangular, trapezoidal, and semi-circular. Sharp-crested weirs have a lower flow potential relative to finite crest length weirs and are typically used in labs and narrow channels [5]. Bagheri and Heidarpour presented a recent analysis on sharp-crested weirs focused on the incorporation of velocity due to free-vortex motion assumed between the upper and lower nappe profiles [6]. Understanding the characteristics of the flow over a sharp-crested weir and its counter-current form does not fully understand.

Open channel flow can be defined as fluid flow with a free open surface to the atmosphere. The transport of sediment has been traditionally described using empirical or semi-empirical formulations

---

\*Corresponding author: [fawzi@uthm.edu.my](mailto:fawzi@uthm.edu.my)

2022 UTHM Publisher. All rights reserved.

[publisher.uthm.edu.my/periodicals/index.php/rpmme](http://publisher.uthm.edu.my/periodicals/index.php/rpmme)

[7]. The example of open channel flow in real life includes the flow in natural river course and artificial open channel [8]. According to the past study, the upstream inlet should be located at a sufficient distance from the weir to let the flow fully develop [9].

In this study, a sharp-crested weir in the open channel was tested with different heights of upstream flow water over the weir and the height of tailwater at the downstream flow. The downstream counter-current at specific tailwater height and the effect of tailwater height on the formation of downstream counter-current on sharp-crested weir flow characteristics has been studied.

## 2. Materials and Methods

The open channel setup in this study was including the open channel itself, sharp-crested weir, and the hydraulic bench. For marker for the visualization and observation of the experiment, a dowel was used. The dowel used comes in a cylindrical shape. This dowel needs to dip in a beaker containing water and mass reading after the dowel takes out from the beaker. The proven observation and the counter-current formation were captured by a high-speed camera. The high-speed camera was equipped with softbox lighting and its tripod stand. Figure 1 shows the full setup of the open channel for the whole experiment.

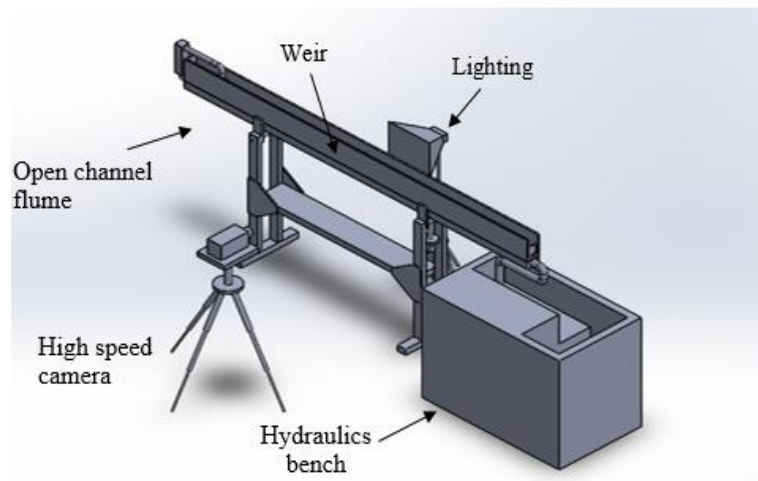


**Figure 1: Equipment setup for the experiment.**

### 2.1 Open channel setup

The sharp-crested weir model was placed at the center of the open channel flume. This can give a length for the water flow from the inlet of the flume to stable before the flow goes through the sharp-crested weir. This is important because the formation of the downstream counter-current will oscillate if the flow from the upstream is not stable. The detail of the sharp-crested weir and its dimension shows in the figure below:

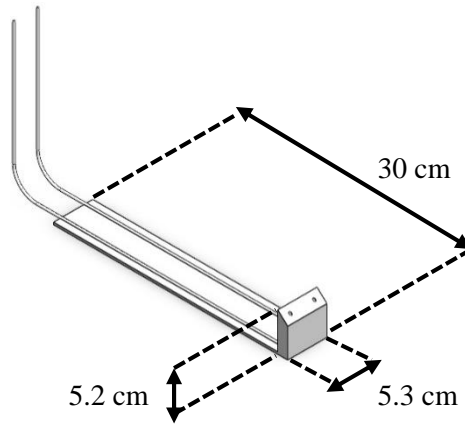


Figure 2: Sharp crested weir from Techquipment brand.

### 3. Results and Discussion

The downstream counter-current existence for flow over sharp-crested weir was observed. Displacement of dowel in the counter-current formation was recorded, and Froude number and velocity in X-direction were calculated. The relationship between upstream head over the sharp-crested and tailwater height on the performance of the counter-current was analyzed.

#### 3.1 Velocity distribution in X-direction on weir downstream

Contour graph plotted by using the velocity distribution in X-direction. The contour graph for the velocity distribution in X-direction was divided into three zones. The first zone, defined as Zone 1, represents the peak of the sharp-crested weir to the entrainment point. For Zone 2, the counter-current zone indicates from the entrainment point to 3.25 coordinates in the longitudinal direction. Lastly, the zone where the dowel exceeds the recovery line and flows to the outlet of the open channel is known as Zone 3. For a positive velocity value, the flow moves away from the weir. The negative velocity value represents the flow of the dowel towards the weir in the counter-current area.

##### 3.1.1 Case 1 and 5

Figure 3 below shows the result of velocity distribution in X-direction obtained from plotted contour graph for the combination of Case 1 and 5 with setup height of flow over the weir ( $h/P$ ) 0.3 and tailwater height ( $t_w/P$ ) 0.8. The velocity in X-direction is calculated and plotted with the coordinate for its velocity using Origin Lab 2019. The information of setup, velocity and the number of the point plotted shown on the graph.

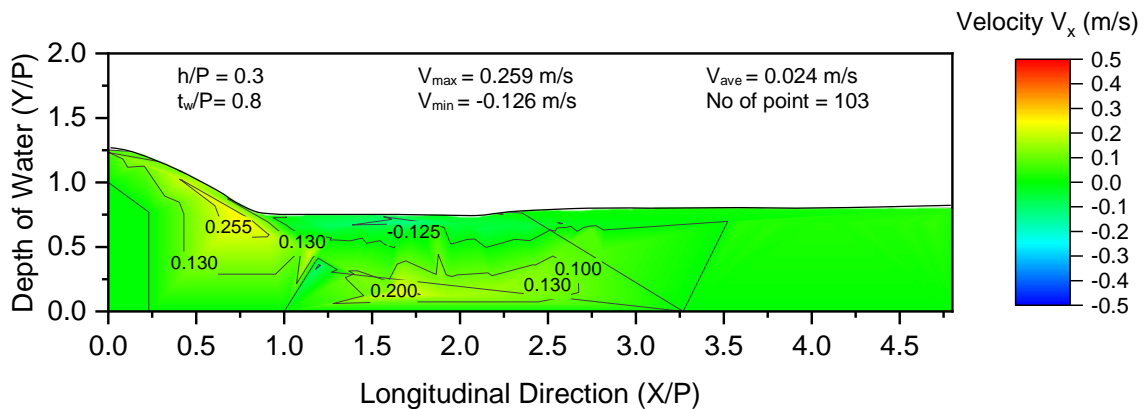
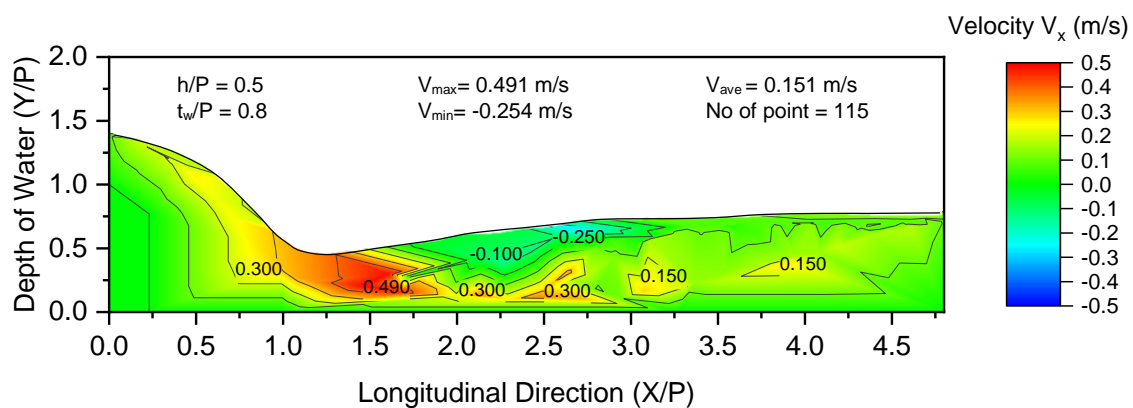


Figure 3: Velocity Distribution in X-direction for ( $h/P$ ) 0.3 and ( $t_w/P$ ) 0.8

Based on the experiment, the contour graph was produced using data for Case 1 and 5 due to the same setup. The contour graph in Figure 3 shows the highest velocity was on the entrainment point between water flows from the upstream to the downstream. The minimum velocity shown in the graph is  $-0.126$  m/s, which is the counter-current velocity. Thus, the range of the velocity distribution in the contour colour scale ranges from  $-0.1$  m/s to  $0.1$  m/s. Next, observation of tailwater height ( $t_w/P$ )  $0.8$  encourage the formation of counter-current with ( $h/P$ )  $0.3$ . Circulation of dowel in the counter-current takes a moment before it can reach Zone 3. The tailwater height use help in the formation of the downstream counter-current.

### 3.1.2 Case 2, 3, 9 and 13

Figure 4 below shows the result of velocity distribution in X-direction obtained from plotted contour graph for the combination of Case 2, 3, 9, and 13 with setup height of flow over the weir ( $h/P$ )  $0.5$  and tailwater height ( $t_w/P$ )  $0.8$ . The velocity in X-direction is calculated and plotted with the coordinate for its velocity using Origin Lab 2019. The information of setup, velocity and the number of the point plotted shown on the graph.



**Figure 4: Velocity Distribution in X-direction for ( $h/P$ )  $0.5$  and ( $t_w/P$ )  $0.8$**

The contour graph was plotted from four cases with the same setup as shown in Figure 4. The higher velocity value was located in Zone 2 with  $0.491$  m/s. This velocity indicates that the dowel passing through the entrainment point and flows in the counter-current zone. The minimum velocity for this case is  $-0.254$  m/s, slightly lower than Case 1 and 5. Therefore, based on the contour graph, the counter-current velocity in X-direction for this case is high.

The tailwater height used in this case was the same as the previous case. Increasing ( $h/P$ ) to  $0.5$  gives a counter-current formation with a higher velocity value. Therefore, it can be concluded that the setup used in this experiment encourages counter-current existence.

### 3.1.3 Case 4

Figure 5 below shows the result of velocity distribution in X-direction obtained from plotted contour graph for the combination of Case 4 with setup height of flow over the weir ( $h/P$ )  $0.6$  and tailwater height ( $t_w/P$ )  $1.0$ . The velocity in X-direction is calculated and plotted with the coordinate for its velocity using Origin Lab 2019. The information of setup, velocity and the number of the point plotted shown on the graph.

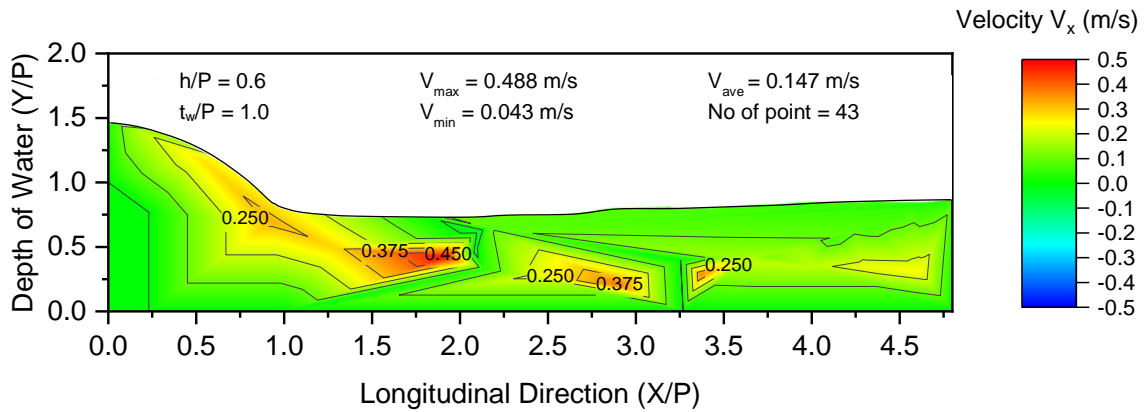


**Figure 5: Velocity Distribution in X-direction for (h/P) 0.6 and (t<sub>w</sub>/P) 1.0**

From the plotted graph above, there is no counter-current existence from the peak of the sharp-crested weir to the downstream outlet. Therefore, the velocity of the dowel flowing from the upstream to the entrainment point is lower than the velocity flow in Zone 2, which is 0.450 m/s.

The value of (h/P) and (t<sub>w</sub>/P) for this case is higher. The yellow scale of velocity located in the graph indicates the velocity value that higher than 0.100 m/s. Increased tailwater height does not affect the counter-current since there are no counter-currents in this case.

3.1.4 Case 6

Figure 6 below shows the result of velocity distribution in X-direction obtained from plotted contour graph for the combination of Case 6 with setup height of flow over the weir (h/P) 0.6 and tailwater height (t<sub>w</sub>/P) 0.7. The velocity in X-direction is calculated and plotted with the coordinate for its velocity using Origin Lab 2019. The information of setup, velocity and the number of the point plotted shown on the graph.

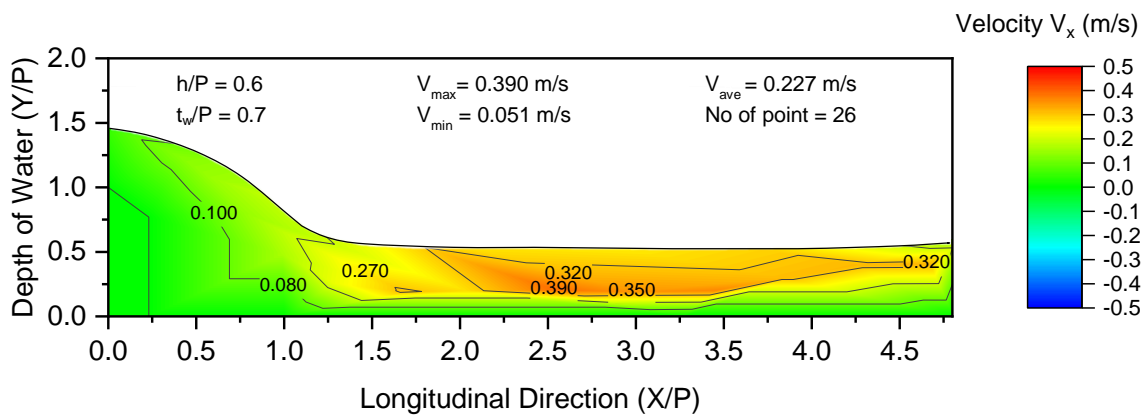


**Figure 6: Velocity Distribution in X-direction for (h/P) 0.6 and (t<sub>w</sub>/P) 0.7**

The contour graph shown in Figure 4.6 shows that the highest velocity is located in zones 2 and 3. The dowel flows smoothly from the inlet to the outlet of the open channel flume without having any counter-current flow. The maximum velocity is found in the middle of Zone 2 with the y-axis (Y/P) 0.25.

In this condition, the flow of the dowel passes through the entrainment point towards the middle depth of the downstream. The velocity of the dowel in this zone is inversely proportional to the depth of water. Therefore, the flow of the dowel to the downstream outlet showed no counter-current when the tailwater height was low.

### 3.1.5 Case 7

Figure 7 below shows the result of velocity distribution in X-direction obtained from plotted contour graph for the combination of Case 7 with setup height of flow over the weir ( $h/P$ ) 0.5 and tailwater height ( $t_w/P$ ) 1.0. The velocity in X-direction is calculated and plotted with the coordinate for its velocity using Origin Lab 2019. The information of setup, velocity and the number of the point plotted shown on the graph.

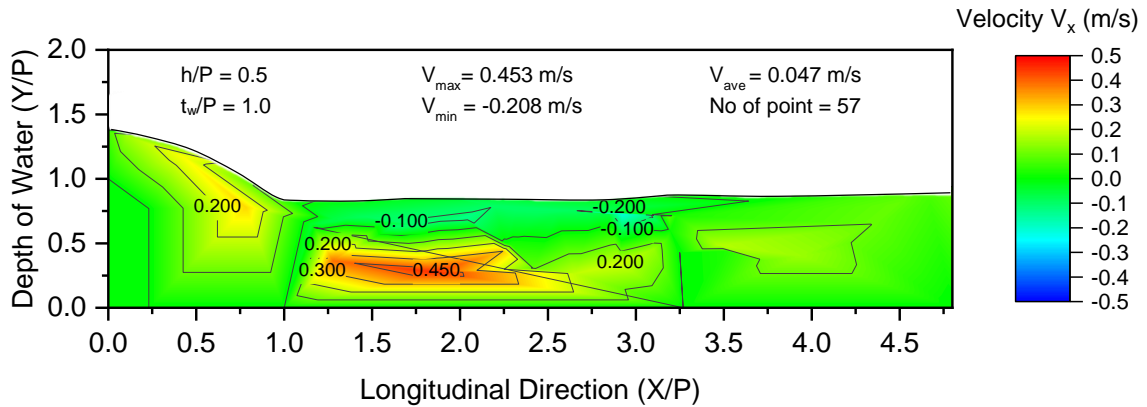


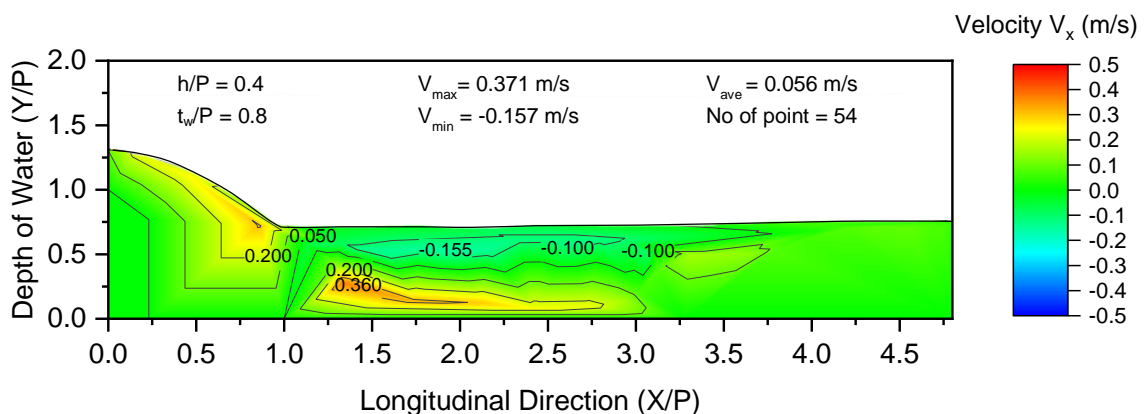
**Figure 7: Velocity Distribution in X-direction for ( $h/P$ ) 0.5 and ( $t_w/P$ ) 1.0**

The formation of counter-current flow can be seen in Zone 2. The counter-current velocity in the graph was  $-0.208$  m/s. The impact velocity of the dowel is located near the entrainment point with  $0.200$  m/s. Next, for the bed current velocity, the maximum value is  $0.453$  m/s. However, there are areas or points in the graphs that revealed the velocity is equal to  $0$  m/s. It was due to the dowel was located at the same coordinate for a short time.

The downstream depth is directly proportional to the tailwater height. It is because the dowel circulates in the counter-current for a moment before it approaching the recovery region. Increasing tailwater height will increase the high of the counter-current region so that the dowel will pull deeper into the downstream region.

### 3.1.6 Case 8

Figure 8 below shows the result of velocity distribution in X-direction obtained from plotted contour graph for the combination of Case 8 with setup height of flow over the weir ( $h/P$ ) 0.4 and tailwater height ( $t_w/P$ ) 0.8. The velocity in X-direction is calculated and plotted with the coordinate for its velocity using Origin Lab 2019. The information of setup, velocity and the number of the point plotted shown on the graph.



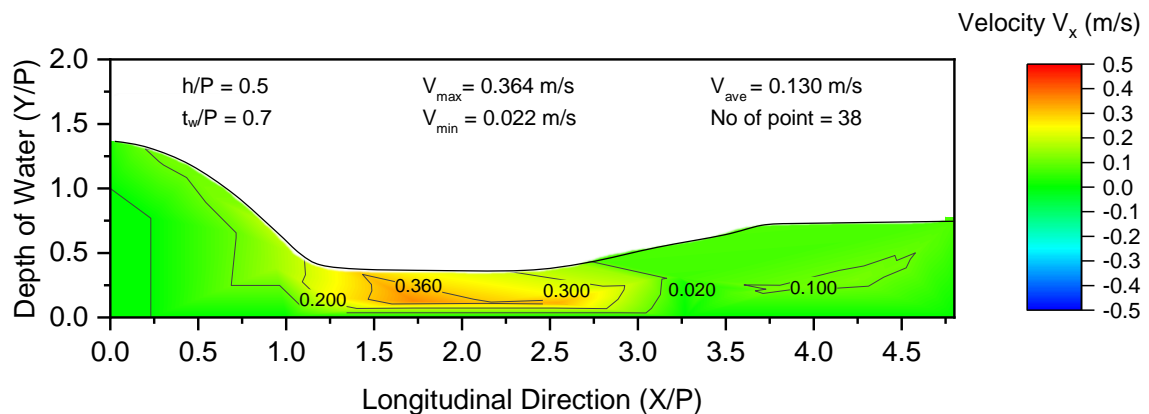
**Figure 8: Velocity Distribution in X-direction for ( $h/P$ ) 0.4 and ( $t_w/P$ ) 0.8**

Figure 8 shows the tabulated velocity distribution for Case 8 with an average velocity of 0.056 m/s. This case was conducted with a flowmeter reading of 20 Lpm to produce (h/P) 0.4. From Zone 1, the impact velocity for the dowel at the entrainment point is 0.200 m/s same as crest velocity. Thus, uniform flow creates a clear boundary for the maximum velocity at the bed current and counter-current velocity region on the graph.

Tailwater depth encourages the formation of counter-current in this case. The higher counter-current velocity shown on the graph is -0.157 m/s. The velocity value near the entrainment point is 0.050 m/s. It is represented by the flows of dowel that circulates for a while in the same coordinate.

### 3.1.7 Case 10

Figure 9 below shows the result of velocity distribution in X-direction obtained from plotted contour graph for the combination of Case 10 with setup height of flow over the weir (h/P) 0.5 and tailwater height (t<sub>w</sub>/P) 0.7. The velocity in X-direction is calculated and plotted with the coordinate for its velocity using Origin Lab 2019. The information of setup, velocity and the number of the point plotted shown on the graph.



**Figure 9: Velocity Distribution in X-direction for (h/P) 0.5 and (t<sub>w</sub>/P) 0.7**

The contour graph for Case 10 is shown in Figure 9, with 38 points plotted for the coordinate and velocity of the dowel. The graph shows the depth of water in Zone 2 lower than the water depth in zone 3. In this case, tailwater height was 0.7, which equal to 36.4 mm. Dowel flow from the upstream to the downstream outlet without experience any counter-current. To obtain the value of (h/P) 0.5, it requires the flow meter reading to exceed 30 Lpm. The average velocity was 0.130 m/s with the maximum 0.364 m/s located in Zone 2 and 0.022 m/s when the dowel reaches the water surface and flows to the downstream outlet.

### 3.1.8 Case 11

Figure 10 below shows the result of velocity distribution in X-direction obtained from plotted contour graph for the combination of Case 11 with setup height of flow over the weir (h/P) 0.3 and tailwater height (t<sub>w</sub>/P) 1.0. The velocity in X-direction is calculated and plotted with the coordinate for its velocity using Origin Lab 2019. The information of setup, velocity and the number of the point plotted shown on the graph.

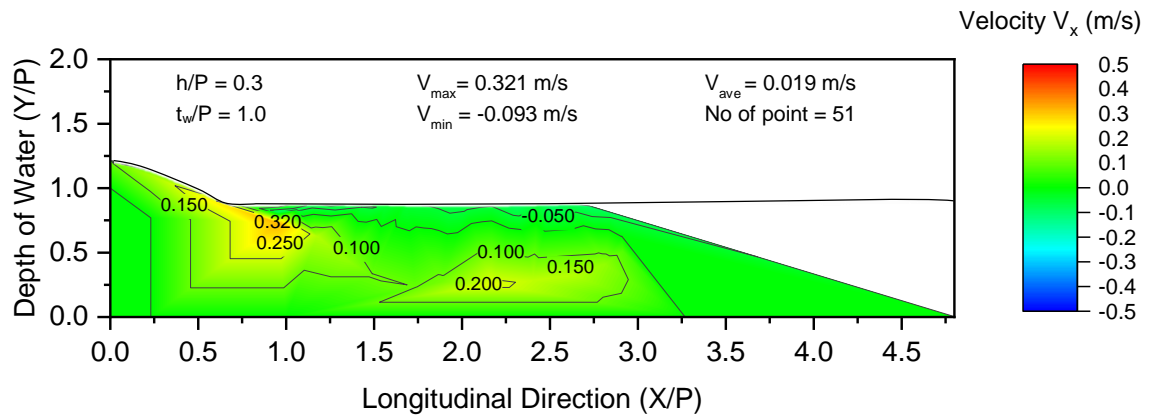


**Figure 10: Velocity Distribution in X-direction for (h/P) 0.3 and (t<sub>w</sub>/P) 1.0**

The result from conducted experiment for Case 11 is illustrated in Figure 10. The plotted contour graph shows the lack of information in analysis for the surface velocity in Zone 3. The limitation for this case to be repeated is due to pandemic Covid-19. Hence students were not allowed to experiment in the lab. However, the existing result for the experiment shows that the repetition of dowel flow in the counter-current without exceeding the recovery line.

From Figure 4.10, the impact velocity for the dowel is high compared to the crest velocity, which is defined as the maximum velocity in this case. The dowel flows through and circulates in Zone 2 caused by the counter-current. The dowel in Zone 2 flows toward the entrainment point after passing through the bed current with a counter-current velocity of -0.093 m/s. Since there is no data for the dowel move toward the downstream outlet, there is no surface velocity in this case.

### 3.1.9 Case 12

Figure 11 below shows the result of velocity distribution in X-direction obtained from plotted contour graph for the combination of Case 12 with setup height of flow over the weir (h/P) 0.4 and tailwater height (t<sub>w</sub>/P) 1.0. The velocity in X-direction is calculated and plotted with the coordinate for its velocity using Origin Lab 2019. The information of setup, velocity and the number of the point plotted shown on the graph.

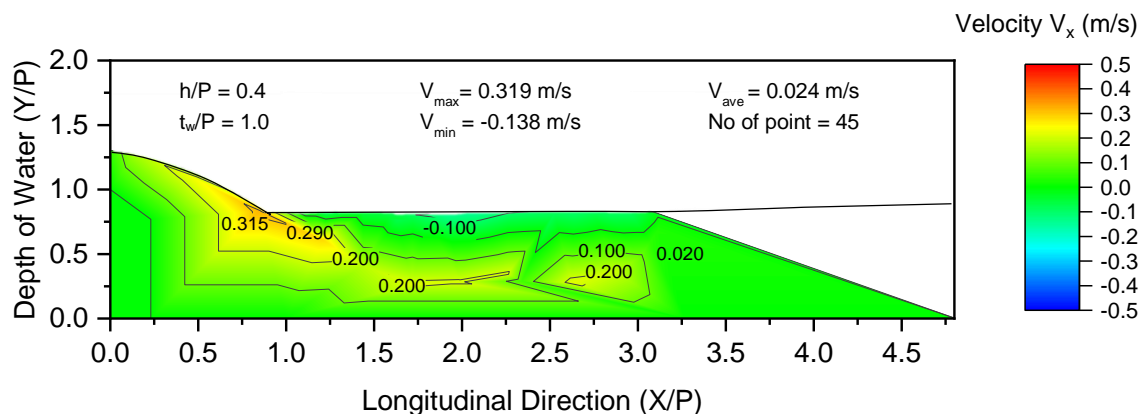


**Figure 11: Velocity Distribution in X-direction for (h/P) 0.4 and (t<sub>w</sub>/P) 1.0**

Due to the Covid-19 pandemic, the Case 12 result also cannot be repeated. Therefore, the analysis is limited to Zone 1 and Zone 2. From the recorded video, the dowel cannot reach Zone 3 due to the lack of time in recording the observation. Furthermore, it caused no result recorded in Zone 3 due to insufficient data to analyze the surface velocity.

From the existing plotted coordinate with velocity distribution contour shown in Figure 12, the maximum velocity of 0.315 m/s located at the collision zone between Zone 1 and 2. The velocity of the dowel increase when the dowel flows reached the entrainment point. The minimum velocity was -0.138 m/s, in which the dowel flows toward the entrainment points in the counter-current.

### 3.1.10 Case 14 and 15

Figure 12 below shows the result of velocity distribution in X-direction obtained from plotted contour graph for the combination of Case 14 and 15 with setup height of flow over the weir ( $h/P$ ) 0.4 and tailwater height ( $t_w/P$ ) 0.7. The velocity in X-direction is calculated and plotted with the coordinate for its velocity using Origin Lab 2019. The information of setup, velocity and the number of the point plotted shown on the graph.

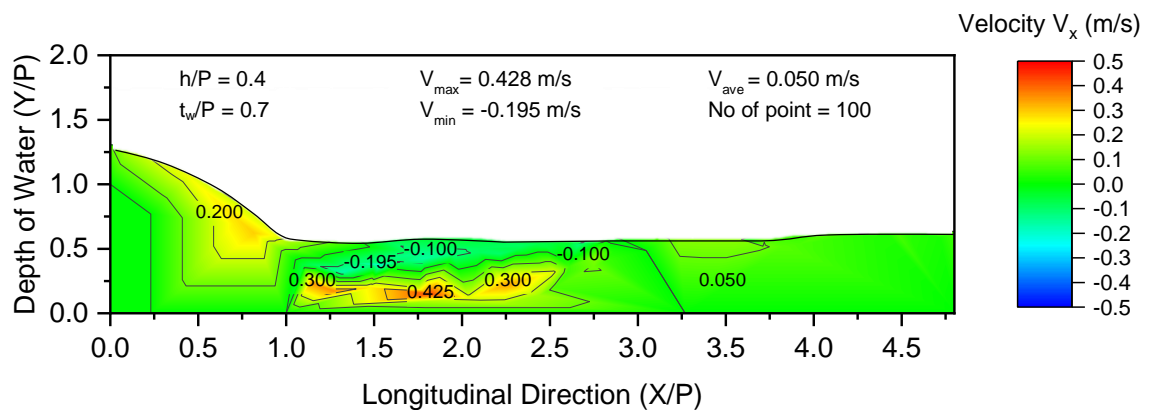


**Figure 12: Velocity Distribution in X-direction for ( $h/P$ ) 0.4 and ( $t_w/P$ ) 0.7**

A combination of Case 14 and 15 plotted in a contour graph. It was due to the same setup of the experiment for ( $h/P$ ) and ( $t_w/P$ ). The combination of 100 points by using digitizer with velocity in X-direction clearly explains that the downstream velocity was high for the dowel. From Figure 12, the dowel experiences the counter-current flow after passing through the maximum velocity in the water. Increasing velocity from the crest can be seen after the dowel meets the entrainment point and continues to the current downstream. The graph showed that the maximum and minimum velocity of the dowel was in Zone 2.

Next, the lower tailwater height ( $t_w/P$ ) is used in this case. Tailwater height setup helps the formation downstream counter-current formation at the. In addition, lower tailwater height encourages the counter-current formation when the upstream flow is low since the flow meter at the upstream reading was 20 Lpm.

### 3.1.11 Case 16

Figure 13 below shows the result of velocity distribution in X-direction obtained from plotted contour graph for the combination of Case 16 with setup height of flow over the weir ( $h/P$ ) 0.6 and tailwater height ( $t_w/P$ ) 0.8. The velocity in X-direction is calculated and plotted with the coordinate for its velocity using Origin Lab 2019. The information of setup, velocity and the number of the point plotted shown on the graph.

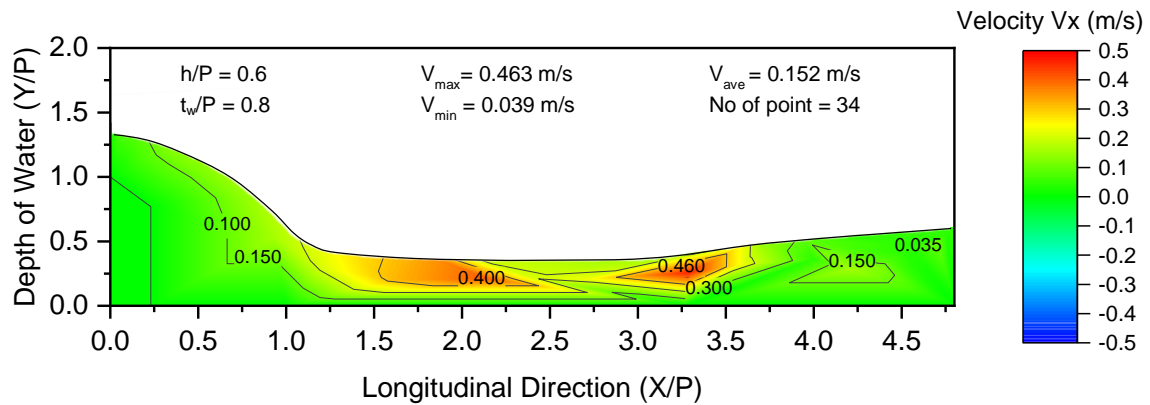


**Figure 13: Velocity Distribution in X-direction for (h/P) 0.6 and ( $t_w/P$ ) 0.8**

Velocity in X-direction from Case 16 was plotted in the figure above. In this conducted experiment, 0.6 for (h/P) is the higher value includes Case 4 6. In comparison to the other cases, it needs an increased flow of water to achieve this value. To obtain (h/P) 0.6, the reading of the flow meter needs to show 36 Lpm.

From the experiment, the dowel flows smoothly passes through the downstream without undergoing counter-current flow despite having high velocity in Zone 2. By referring to the contour graph above, crest and surface velocity produce nearly the same velocity. It can be concluded that the dowel velocity decreases after it flows through Zone 2. Tailwater height used in this case does not contribute to the formation of counter-current. High flow from the upstream hinders the counter-current formation since the tailwater height was not enough.

#### 4. Conclusion

This study successfully introduced the downstream counter-current of an open channel with the different upstream and downstream water levels. The method used in the experiment was simple and easy to handle regarding open channel flume, hydraulic bench, Rengas dowel as flow visualization marker, and high-speed camera to record the counter-current formation. Based on the experimental result, the objective of this study was achieved.

- i. The flow height over the weir is directly proportional to the tailwater height. Investigation through the experiment shows that the water level on the upstream (h/P) and tailwater height ( $t_w/P$ ) encourages the counter-current formation. Thus, the upstream water level plays a significant role in controlling the size of the counter-current. It is because the flow from the upstream controls the flow through the downstream region.
- ii. Higher tailwater will increase the downstream depth tend to the formation of the counter-current. Low tailwater height at the downstream, with high flow height over the weir, can prevent the formation of downstream counter-current
- iii. The downstream zone is divided into two sections: counter-current and bed current. The velocity of flow in the bed current region is faster than in the counter-current region. Therefore, a higher velocity identified when the dowel entered Zone 2 with the range distance is between the entrainment and middle regions.

#### Acknowledgement

The authors would also like to thank the Faculty of Mechanical and Manufacturing Engineering, Universiti Tun Hussein Onn Malaysia for its support.

## References

- [1] J. Ren, A. Zhang, and X. Wang, "Journal Pre," *Pharmacol. Res.*, p. 104743, 2020, doi: 10.1016/j.flowmeasinst.2020.101867.
- [2] A. Ferrari, "SPH simulation of free surface flow over a sharp-crested weir," *Adv. Water Resour.*, vol. 33, no. 3, pp. 270–276, 2010, doi: 10.1016/j.advwatres.2009.12.005.
- [3] R. J. Olsen, M. C. Johnson, and S. L. Barfuss, "Risk of Entrapment at Low-Head Dams," *J. Hydraul. Eng.*, vol. 139, no. 6, pp. 675–678, 2013, doi: 10.1061/(asce)hy.1943-7900.0000721.
- [4] B. A. Tschantz and K. R. Wright, "Hidden dangers and public safety at low-head dams," *J. Dam Saf.*, vol. 9, no. 1, pp. 8–17, 2011.
- [5] S. Salehi, K. Esmaili, and A. H. Azimi, "Mean velocity and turbulent characteristics of flow over half-cycle cosine sharp-crested weirs," *Flow Meas. Instrum.*, vol. 66, no. November 2017, pp. 99–110, 2019, doi: 10.1016/j.flowmeasinst.2019.02.002.
- [6] S. Bagheri and M. Heidarpour, "Flow over rectangular sharp-crested weirs," *Irrig. Sci.*, vol. 28, no. 2, pp. 173–179, 2010, doi: 10.1007/s00271-009-0172-1.
- [7] M. Ahadi, D. J. Bergstrom, and K. A. Mazurek, "Application of the two-fluid model to prediction of sediment transport in turbulent open channel flow," *Phys. Chem. Earth*, vol. 113, no. September 2018, pp. 73–82, 2019, doi: 10.1016/j.pce.2019.06.001.
- [8] R. Xu and S. Liu, "Level Set method-based two-dimensional numerical model for simulation of nonuniform open-channel flow," *PLoS One*, vol. 14, no. 9, pp. 1–18, 2019, doi: 10.1371/journal.pone.0223167.
- [9] H. Saadatnejadgharahassanlou, R. I. Zeynali, A. Gharehbaghi, S. Mehdizadeh, and B. Vaheddoost, "Three dimensional flow simulation over a sharp-crested V-Notch weir," *Flow Meas. Instrum.*, vol. 71, no. December 2019, p. 101684, 2020, doi: 10.1016/j.flowmeasinst.2019.101684.